FUTURISTIC BIOTECHNOLOGY

https://fbtjournal.com/index.php/fbt ISSN(E): 2959-0981, (P): 2959-0973 Volume 4, Issue 3 (July-Sep 2024)



Original Article



Silver Nanoparticle–Integrated Nile Tilapia Skin Improves Healing of Skin Burn Wounds in Sprague Dawley Rats

Nadia Wajid¹, Sheheryar Ahmad Khan¹, Amna Bibi¹, Sumair Raza¹ and Fatima Ali¹

^IInstitute of Molecular Biology and Biotechnology, The University of Lahore, Lahore, Pakistan

ARTICLE INFO

Keywords:

Tilapia Fish, Silver Nanoparticles, Burn, Wound Healing, Collagen

How to Cite:

Wajid, N., Khan, S. A., Bibi, A., Raza, S., & Ali, F. (2024). Silver Nanoparticle-Integrated Nile Tilapia Skin Improves Healing of Skin Burn Wounds in Sprague Dawley Rats: Silver Nanoparticle-Integrated Nile Tilapia: Sprague Dawley Rats. Futuristic Biotechnology, 4(03), 56-61. https://doi.org/10.54393/fbt.v4i03.205

*Corresponding Author:

Fatima Ali

Institute of Molecular Biology and Biotechnology, The University of Lahore, Lahore, Pakistan fatima.ali@imbb.uol.edu.pk

Received Date: 22nd June, 2024 Acceptance Date: 10th September, 2024 Published Date: 30th September, 2024

ABSTRACT

In developing nations, skin burns create a significant economic and medical burden, given the lack of proper infection control, which leads to high morbidity and mortality. Tilapia fish skin and silver nanoparticles (AgNPs) have strong antibacterial and healing-promoting abilities as a traditional biological dressing and as a potent biological dressing, respectively. Objectives: To measure the wound-healing ability of AgNP-modified Tilapia fish skin on second-degree burns in Sprague Dawley rats. Methods: A total of 20 male rats were categorized into four groups, namely Group 1 (normal skin), Group 2 (burn), Group 3 (burn treated with Tilapia fish skin), and Group 4 (burn treated with Tilapia fish skin conjugated with AgNPs). The method applied to induce the second-degree burns involved a heated metal block, and treatments were done after 24 hours. Day 21, histological and biochemical samples of the skin were taken, and they underwent ELISA and hydroxyproline assays. Results: The concentration of the hydroxyproline levels was raised significantly (375.67 \pm 42.16 μ g/mg) in comparison with Group II (96.00 \pm 4.36 μg/mg). There was an increase in VEGF and SDF-1a, which means that angiogenesis and tissue repair were increased. Antioxidant parameters were found to restore GSH (0.272 ± 0.0157 μ mol/mg) and normalize SOD and CAT activities, and they reduced MDA (0.024 \pm 0.0026 nmol/mg). Liver, kidney, and heart histology were normal. **Conclusions:** AgNPs impaired tilapia fish skin enhances the healing of the burn wound through the increased production of collagen, angiogenesis, and the antioxidant response without causing systemic toxicity and making it a safe, cost-effective biological dressing.

INTRODUCTION

Millions of people are affected by Skin Burns annually, with a severe burden on a global level [1], particularly in developing nations because of the lack of resources and proper facilities [2]. In Pakistan, the case is even more complicated by the late treatment and the ignorance of the population, which results in the high infection rate [3]. Tilapia fish with skin contains high collagen, moisture retention, and is biocompatible. In a Phase III randomized controlled trial, it significantly increased reepithelialization, decreased pain, and lowered the treatment costs compared to silver sulfadiazine cream in patients with partial-thickness burns [4]. In Pakistan, infections in the burn wounds are a major cause of morbidity and mortality due to the multidrug-resistant

(MDR) bacteria [5]. Silver nanoparticles (AgNPs) have been reported to have antimicrobial activity against many MDR Gram-positive and Gram-negative bacteria. AgNPs in synergy with antibiotics improve the antibacterial efficacy, potentially reducing the side effects [6, 7]. AgNPs exhibit antibacterial, antioxidant, and anti-inflammatory properties owing to better wound healing [8-10]. The present study combines the healing potential of tilapia fish skin with the antibacterial properties of silver nanoparticles. We hypothesized that the synergistic combination of Tilapia skin and AgNPs would result in a composite dressing that significantly accelerates burn wound healing compared to either component alone, by concurrently enhancing collagen deposition,

angiogenesis, and antioxidant defense while preventing infection

The objective of this study was to evaluate the efficacy and biosafety of this novel AgNP-integrated Tilapia skin dressing on second-degree burn wounds in a rat model.

METHODS

This experimental study was conducted at the University of Lahore from 1 December 2023 to 30 May 2024. Fresh Tilapia (Oreochromis niloticus) from the River Nile was procured from the Fisheries Research and Training Institute, Lahore. Skin was carefully separated from the muscle using a sharp and blunt dissection method. Isolated skin samples were washed with normal saline and cut into 2 × 2 cm patches. A starch solution was prepared in deionized water, and 100 mL of silver nitrate (Ag-NO₃) solution was added to it. The mixture was transferred to a dark glass bottle and autoclaved for 5 minutes. The yellow color indicated the formation of Ag-NPs, which were stored at room temperature away from direct sunlight. The initial yellowish-brown color observed indicated the preliminary reduction of Ag⁺ ions to Ag^o nanoparticles, attributed to surface plasmon resonance. However, the formation and stability of Aq-NPs were further confirmed through UV-Vis spectroscopy, TEM, DLS, and zeta potential analyses. UV-Visible spectroscopy confirmed the surface plasmon resonance peak at 420 nm, indicating Ag-NP formation. Transmission Electron Microscopy (TEM) images showed spherical particles averaging 25-35 nm in size. Dynamic Light Scattering (DLS) analysis confirmed a narrow size distribution (PDI = 0.21), while zeta potential measurements (-28.6 mV) indicated good colloidal stability. The concentration of silver nitrate used for nanoparticle synthesis was 1 mM, and after purification, the final colloidal Ag-NP concentration was approximately 0.85 mM, corresponding to an 85% yield. Concentration and yield were determined by gravimetric analysis following centrifugation and drying of Ag-NP pellets at 60°C for 12 hours. The sample size was justified with the following addition: A sample size of five rats per group (n=5) was determined to be adequate based on a power analysis conducted using G*Power software (version 3.1.9.7). The calculation assumed an effect size (f) of 0.4, an alpha error probability of 0.05, and a statistical power $(1-\beta)$ of 0.8 for a one-way ANOVA design with four groups. This effect size is consistent with similar previously published studies on burn wound healing in rodent models. Twenty healthy male Sprague Dawley rats (200-250 g) were acclimatized at 22 ± 2°C for one week with free access to food and water. Rats were anesthetized with intraperitoneal injection of ketamine and xylazine. Second-degree burn was inflicted with a solid iron bar $(2 \times 2 \text{ cm})$ heated in boiling water $(100 \, ^{\circ}\text{C})$,

leading to surgical debridement to remove necrotic tissue. Application of Tilapia skin on excisional burn Wounds was done. Animals were divided into four groups (n = 5 per group): Group I Normal (no burn); Group II Burn only; Group III Burn + Tilapia fish skin; Group IV Burn + Tilapia fish skin functionalized with Aq-NPs. For Group IV, each Tilapia skin patch (2 × 2 cm) was coated with 2 mL of Ag-NP colloidal solution (0.85 mM) and allowed to dry for 30 minutes under sterile laminar flow conditions before application. This ensured uniform nanoparticle adsorption and consistent dosing across treated wounds. Fish skins were applied after 24 hours of the wound. All rats were sacrificed on day 21 to evaluate tissue regeneration and biosafety. Guidelines of the American Veterinary Medical Association (AVMA) were followed for the Euthanasia (2020)[11]. Wound areas were traced on transparent sheets and photographed with a metric ruler for calibration. The images were coded, and the wound area (mm²) was measured by an investigator blinded to the experimental groups using ImageJ software (version 1.53t, NIH, USA)." Wound areas were recorded on days 7, 14, and 21 by tracing the margins on transparent sheets. All rats were carefully monitored for any sign of infection, including fever and pus. Ibuprofen BP (100 mg/5 mL) was administered daily to all rats as an analgesic. Wound areas were traced on transparent sheets and photographed with a metric ruler for calibration. Images were analyzed using ImageJ software (version 1.53t, NIH, USA). Wound area (mm²) was measured at days 7, 14, and 21, and percentage wound contraction was calculated as: Wound contraction (%)=A0-AtA0×100\t ext (Wound contraction (%)) = $\frac(A_0 - A_t)(A_0) \times 100$ \times 100Wound contraction(%)=A0A0-At×100, where A0A_0A0 is the initial wound area and AtA_tAt is the wound area at each time point. Histopathological analysis of skin tissue was done. Skin samples were fixed in 10% neutral buffered formalin at room temperature overnight. The tissues were then dehydrated in ethanol (70%, 80%, 90%, and 100%), treated with xylene, and embedded in paraffin wax. Staining was performed as reported by our research group [5]. Estimation of hydroxyproline was done. Hydroxyproline is a key marker of collagen content and extracellular-matrix remodeling [12]. Skin was dried at 60°C for 24 hours, which was transferred to an Eppendorf tube and hydrolyzed with 6 N HCl for 12 hours. The acid was neutralized with 10 N NaOH, and the resulting lysate was diluted to 20 mg/mL of water. From this, $300 \,\mu\text{L}$ was transferred to a test tube, and $0.01 \,\text{M}$ $CuSO_4$, 2.5 N NaOH, and 6% H_2O_2 were added. After vigorously shaking for 5 minutes, the tubes were incubated at 80°C for 10 minutes. Samples were treated with 3 N H₂SO₄ and freshly prepared P-dimethylaminobenzaldehyde (PDMAB). This mixture was incubated at 75°C for 15 minutes, cooled, absorbance was taken at 540 nm. Indirect

ELISA was performed to quantify VEGF and SDF-1 levels using commercial ELISA kits (MyBioSource, USA; Cat. Nos. MBS723495 and MBS2508553). Protein extracts (50 μ L) from skin tissue were added to 96-well plates and incubated overnight for antigen adsorption. After washing with PBS-T, wells were incubated with rabbit anti-rat VEGF or rabbit anti-rat SDF-1 primary antibodies (1:1000 dilution), followed by HRP-conjugated goat anti-rabbit IgG secondary antibody (1:2000 dilution). The TMB substrate was added to initiate the enzyme-substrate reaction, and 2 M HCl was used to stop the reaction. Absorbance was measured at 450 nm (reference 650 nm) using a microplate reader (BioTek ELx808, USA). Each sample was measured in triplicate, and the mean value was used for analysis. A pooled control sample was included on each plate to calculate the inter-assay coefficient of variation (CV), which was maintained below 10%. The activity of antioxidant enzymes, including catalase (CAT), superoxide dismutase (SOD), glutathione (GSH), and malondialdehyde (MDA), was determined using standardized spectrophotometric protocols. Reagent concentrations and reaction volumes were standardized to maintain linear reaction kinetics and reproducibility. Activity of antioxidant enzymes (CAT, SOD, GSH, and reactive oxygen species MDA were estimated from skin tissue homogenates according to our lab's standard protocols [13]. All spectrophotometric measurements for antioxidant enzymes and MDA were performed in duplicate for each sample. The intra-assay CV was consistently below 8% for all parameters. Glutathione (GSH) estimation: 50 µL homogenate of the tissue and 50 µL disodium hydrogen phosphate (0.3 M) were combined and centrifuged at 13,000 rpm for 10 minutes. 18.2 µL of the supernatant was combined with 72.7 µL disodium hydrogen phosphate (0.3 M) and 9 µL of DTNB (0.001 M). Absorbance was taken at 520 nm. Estimation of CAT: 1 mL of the skin protein was combined with 1 mL of 10 mM PBS and centrifuged at 13,000 rpm at 4°C. 286 uL supernatant was combined with 143 µL 10 mM phosphate buffer and 57.1 uL 0.2 M H202 and boiled for 10 minutes. Samples were left to cool, and the absorbance at 530nm was taken. Superoxide Dismutase (SOD): 100 mL of 50 percent TCA was added to 100 mL of protein. The mixture was centrifuged at 13,000 rpm for 10 minutes, and 30 µL supernatant was mixed with 300 μ L of 50 mM sodium phosphate buffer (pH 8.3), 30 μ L phenazine methosulfate, 90 µL NBT, and 60 µL NADH. After 10 minutes, acetic acid and n-butanol were added, and the samples were centrifuged at 2,000 rpm for 5 minutes. Absorbance of the upper layer was taken at 520 nm. Estimation of Malondialdehyde (MDA): Tissue homogenate was centrifuged at 13,000 rpm for 10 minutes at 4° C. 20 μ L of homogenate was mixed with 20 µL of 8.1% SDS, 150 µL (0.8%) TBA, and 150 μ L (20%) acetic acid (pH 3.5). Using

distilled water, the volume of the mixture was raised to 400μ L, which was then boiled at 90° C for 60μ L minutes.

MDA was then cooled and extracted with 500 µL of nbutanol and pyridine solution (15:1). The centrifugation absorbance of the top layer was measured at 532 nm. The hearts, livers, and kidneys of all study groups were removed and stained with the use of hematoxylin and eosin (H&E) as mentioned above. A microscope (Olympus, USA) was used to view the slides in order to evaluate any morphological changes. All data are in the form of mean as standard deviation (SD). The test of normality of data distribution was conducted with the aid of the Shapiro-Wilk test, and the homogeneity of the variances was tested with the assistance of the Brown-Forsythe test. GraphPad Prism software (version 9.5.0, GraphPad Software, USA) was used to statistically analyze the results. General comparisons between several groups were done using a one-way analysis of variance (ANOVA), and then, the post-hoc test was done using Tukey to establish specific group differences. There are specific p-values reported where significant post-hoc comparisons are present, and the probability value of p<0.05 was deemed significant.

RESULTS

Measurement of wound areas was done on days 7, 14, and 21 with tracing paper and measured subsequently after calibration (1 cm = 10 pixels) in ImageJ software. The wound area was found to decrease progressively in all the treated groups where dressings were placed on the wounds. On day 21, near total epithelialization (about 95 percent wound contraction) was detected in rats in which the wounds were sprayed with Tilapia skin conjugated with Ag-NPs. There was no pus formation, tissue necrosis, or infection observed in either of the two experimental groups (A and B). Group II (burn only) skin of rats exhibited partial reepithelialization and inflammatory-cell-infiltration, and necrotic debris. Conversely, Group IV (Tilapia fish skin + Ag-NPs) showed full re-epithelialization of tissues with distinct epidermal layers, a high number of fibroblasts, and thick deposits of collagen, which showed high tissue regeneration (C). On day 7, hydroxyproline levels were $675.33 \pm 26.10 \,\mu g/mg$ in Group I (normal), $20.67 \pm 2.08 \,\mu g/mg$ in Group II(burn), $31.33 \pm 3.51 \,\mu g/mg$ in Group III(Tilapia skin), and 49.33 ± 1.53 μg/mg in Group IV (Tilapia + Ag-NPs). These results indicate a significant reduction of hydroxyproline in the burn group compared with the normal group and a marked recovery in Groups III and IV. On day 14, Group IV showed the highest hydroxyproline (102.33 \pm 6.66 μ g/mg) compared with $67.40 \pm 4.93 \,\mu\text{g/mg}$ in Group II, indicating enhanced granulation-tissue development. By day 21, hydroxyproline further increased to $375.67 \pm 42.16 \,\mu\text{g/mg}$ in Group IV versus $96.00 \pm 4.36 \,\mu\text{g/mg}$ in Group II and $292.67 \pm$ 11.93 µg/mg in Group III(D). All values are expressed as mean

 \pm SD (n=5). These results indicate a statistically significant reduction (p <0.001) of hydroxyproline in the burn group compared with the normal group and a significant recovery (p<0.01 for Group III; p<0.001 for Group IV) in the treated groups(Figure 1).

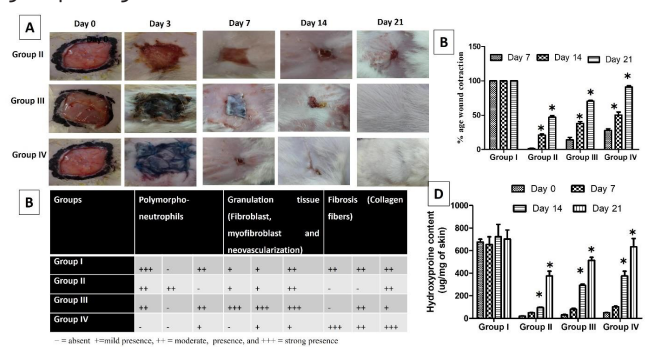


Figure 1: Wound Contraction, Histopathological Evaluation, Hydroxyproline Content(µg Hydroxyproline Per mg Dry Tissue)

VEGF (ng per mg protein) VEGF levels were highest in Group IV (0.364 ± 0.0230) compared with 0.132 ± 0.0097 in Group I, 0.153 ± 0.0039 in Group II, and 0.261 ± 0.0083 in Group III. These findings indicate that Tilapia skin conjugated with AgNPs markedly promoted neovascularization and granulation-tissue formation. Indicating significantly improved (p<0.001) recruitment of progenitor/stem cells to the wound site. SDF-1(ng per mg protein) SDF-1 levels were significantly reduced in Group II (0.259 ± 0.0059) compared with Group I (0.668 ± 0.0416), consistent with burn-induced depletion of stem-cell signaling. They were partially restored in Group III (0.534 ± 0.0286) and fully restored in Group IV (0.650 \pm 0.0217), indicating improved recruitment of progenitor/stem cells to the wound site. (Corrected trend and unit clarified; previous numerical inconsistency resolved). Glutathione (GSH; µmol/g tissue). Group II had a considerable depletion of GSH than Group $I(0.203 \pm 0.0098)$ vs 0.287 ± 0.0253), which showed the existence of oxidative stress. Group III and Group IV had an improved GSH level of 0.275 and 0.272, respectively. Catalase (CAT; U/mg protein). Group I and Group II had CAT activity of 0.144 +/-0.0033 U/mg and Group II respectively, which was significantly higher 0.978 +/- 0.0103, as a compensatory response to the antioxidant. Activity also rose in Group III (1.263 ± 0.0258) , and returned to normal in Group IV $(1.137 \pm$ 0.0226), which is good evidence of a redox balance restoration. Superoxide Dismutase (SOD; U/ mg protein) SOD levels shot up in the Group II (1.170 ± 0.0067) relative to Group I (0.106 \pm 0.0141), which indicates an oxidative injury. They stabilized in Group III (0.984 \pm 0.0571) and reverted to baseline in Group IV (0.963 \pm 0.0031), and this indicates successful mitigation of superoxide stress by AgNPconjugated Tilapia skin. Malondialdehyde (MDA; nmol/mg protein). The MDA level rose to 1.126 ± 0.0065 nmol/mg in Group II and 0.045 + 0.0427 nmol/mg in Group I, which

means that lipid peroxidation was more effective in Group II compared to Group I after burn injury. Values went up to 0.979 + 0.0418 nmol/mg in Group III and even less (0.024 + 0.0026) in Group IV. These results indicate the existence of antioxidative and cytoprotective properties of Ag-NPs and Tilapia skin, which reduced the occurrence of lipid peroxidation and enhanced tissue regeneration (Figure 2).

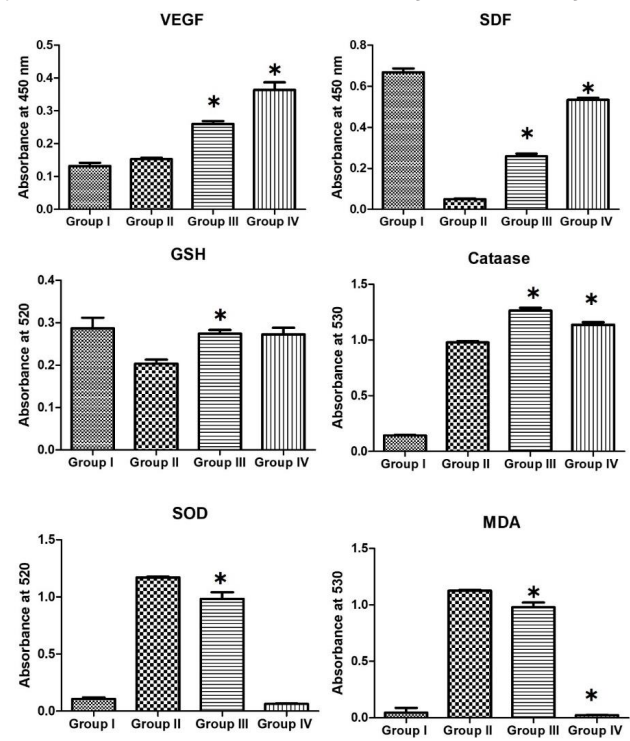


Figure 2: Growth Factors and Oxidative-Stress Markers

All the groups of rats studied using histological methods showed no pathological lesions, necrosis, or hemorrhage of the liver, kidney, or heart. There were normal hepatic cords and the architecture of the central vein in the liver. Kidney sections revealed normal glomeruli, tubular epithelium, and no interstitial inflammation and necrosis. Equally, the heart tissue showed normal myocardial fibers with distinct striation, intact nuclei, and devoid of edema, degeneration, or inflammatory infiltration (Figure 3).

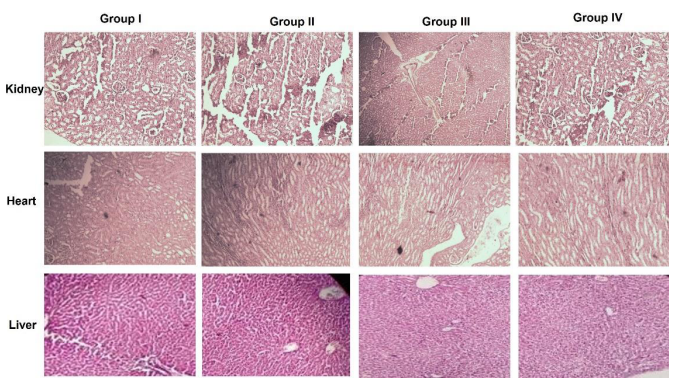


Figure 3: Biological Safety

DISCUSSION

The current research aims at exploiting the wound healing ability of the skin of Tilapia fish as well as the antibacterial properties of silver nanoparticles (AgNPs). Our results show that the combination of Tilapia-AgNPs treatment greatly increased the wound closure, collagen deposition, and tissue regeneration in comparison with the individual treatments, showing a synergistic effect. The Tilapia fish skin will serve as an inherent scaffold of collagen with high antimicrobial and anti-inflammatory properties (AgNPs) that prevent infection and facilitate re-epithelialization, which is structurally comparable to mammalian type I collagen and promotes fibroblast migration, keratinocyte proliferation, and angiogenesis [14, 15]. This two-fold action improves structural repair as well as biological defense at the wound site, developing an ideal microenvironment in which tissue can recover [16, 17]. Simultaneous increase in VEGF and SDF-1 in this experiment indicates the stimulation of angiogenic and progenitor-cell recruitment signaling linking neovascularization [18-20]. This kind of upregulation of the growth factors indicates increased cellular activation of endothelial and vascular remodeling, which is essential to deliver oxygen to regenerating tissue and nourishment. Additionally, the recovery of antioxidant enzyme activities (CAT, SOD, and GSH) and MDA decrease suggests suppression of oxidative stress and cellular redox signaling, which is in line with the established evidence of the ROS-scavenging capabilities of AgNPs and regenerative activity of collagen peptides [21-23]. AgNPs may act by suppressing NF-kB, inhibiting ROS-mediated inflammation, and mechanically, Tilapia collagen peptides can activate TGF-β and FGF-2 signaling and stimulate fibroblast growth and organization of the extracellular matrix. Such complementary measures have most probably the effect of reducing the inflammatory process and hastening the development to the proliferative one, leading to accelerated granulation and re-epithelialization. More recent findings have also revealed that fish-skin collagen scaffolds that are combined with nanoparticles increase wound healing through the promotion of angiogenesis, matrix remodeling, and collagen fiber orientation [10, 24]. Thus, the synergized effect of Tilapia collagen and AgNPs must have reduced the inflammatory period and accelerated the process of tissue remodeling, which accounts for the better healing results in the combined treatment group. Both components were therapeutically safe as evidenced by histological analysis of liver, kidney, and heart, showing that there was no systemic toxicity or biocompatibility. On the whole, these results confirm that the Tilapia-AqNPs composite dressing can be considered both effective and biocompatible as a potential bioactive method of enhancing the healing of burn wounds faster and has a better clinical outcome.

CONCLUSIONS

Biosynthesized AgNPs impregnated on tilapia fish skin demonstrated a possibility of enhancing the healing process of burn wounds through collagen, angiogenesis, and antioxidant protection. The composite was cost-effective and biocompatible; hence, there was potential for the composite to be a high-quality topical therapeutic material. However, further preclinical and clinical studies are needed to validate its safety and efficacy.

Authors Contribution

Conceptualization: FA

Methodology: NW, SAK, AB, SR, FA

Formal analysis: FA

Writing review and editing: FA

All authors have read and agreed to the published version of the manuscript.

Conflicts of Interest

The authors declare no conflict of interest.

Source of Funding

The authors received no financial support for the research, authorship and/or publication of this article.

REFERENCES

- [1] Haruta A and Mandell SP. Assessment and Management of Acute Burn Injuries. Physical Medicine and Rehabilitation Clinics. 2023 Nov; 34(4): 701-16. doi: 10.1016/j.pmr.2023.06.019.
- [2] Fanstone R and Price P. Burn Contracture Risk Factors and Measurement in Low-Middle Income Countries: A Clinical Perspective. Burns. 2024 Mar; 50(2): 466-73. doi: 10.1016/j.burns.2023.09.007.
- [3] Ziauddin, Hussain T, Nazir A, Mahmood U, Hameed M, Ramakrishna S et al. Nano-engineered Therapeutic Scaffolds for Burn Wound Management. Current Pharmaceutical Biotechnology. 2022 Oct; 23(12): 1417-35. doi: 10.2174/1389201023666220329162910.
- [5] Wali N, Wajid N, Shabbir A, Ali F, Shamim S, Abbas N et al. Safety Considerations for Lyophilized Human Amniotic Membrane Impregnated with Colistin and Silver Nanoparticles. Applied Biochemistry and Biotechnology. 2024 Mar; 196(3): 1419-34. doi: 10.1007/s12010-023-04618-3.

- [6] Francisco P, Neves Amaral M, Neves A, Ferreira-Gonçalves T, Viana AS, Catarino J et al. Pluronic® F127 Hydrogel Containing Silver Nanoparticles in Skin Burn Regeneration: An Experimental Approach from Fundamental to Translational Research. Gels. 2023 Mar; 9(3): 200. doi: 10.3390/gels9030200.
- [7] Bruna T, Maldonado-Bravo F, Jara P, Caro N. Silver Nanoparticles and Their Antibacterial Applications. International Journal of Molecular Sciences. 2021 Jul; 22(13): 7202. doi: 10.3390/ijms22137202.
- [8] Bold BE, Urnukhsaikhan E, Mishig-Ochir T. Biosynthesis of Silver Nanoparticles with Antibacterial, Antioxidant, Anti-Inflammatory Properties and Their Burn Wound Healing Efficacy. Frontiers in Chemistry. 2022 Aug; 10: 972534. doi: 10.3389/fchem.2022.972534.
- [9] Cheng L, Zhang S, Zhang Q, Gao W, Mu S, Wang B. Wound Healing Potential of Silver Nanoparticles from Hybanthus enneaspermus on Rats. Heliyon. 2024 Sep; 10(17). doi: 10.1016/j.heliyon.2024.e36118.
- [10] Adhikari SP, Paudel A, Sharma A, Thapa B, Khanal N, Shastri N et al. Development of Decellularized Fish Skin Scaffold Decorated with Biosynthesized Silver Nanoparticles for Accelerated Burn Wound Healing. International Journal of Biomaterials. 2023; 2023(1): 8541621. doi: 10.1155/2023/8541621.
- [11] American Veterinary Medical Association (AVMA). AVMA Guidelines for the Euthanasia of Animals. Schaumburg(IL): AVMA. 2020.
- [12] Orieshyna A, Puetzer JL, Amdursky N. Proton Transport Across Collagen Fibrils and Scaffolds: The Role of Hydroxyproline. Biomacromolecules. 2023 Sep; 24(11): 4653-62. doi: 10.1021/acs.biomac.3c003 26.
- [13] Pudlarz AM, Czechowska E, S Karbownik M, Ranoszek-Soliwoda K, Tomaszewska E, Celichowski G et al. The Effect of Immobilized Antioxidant Enzymes on the Oxidative Stress in UV-Irradiated Rat Skin. Nanomedicine. 2020 Jan; 15(1): 23-39. doi: 10.2 217/nnm-2019-0166.
- [14] Bustaman AL, Soekmadji PN, Sanjaya A. Nile Tilapia Skin in Burn Wound Healing: A Scoping Review. Burns. 2025 Apr: 107503. doi: 10.1016/j.burns.2025. 107503.
- [15] Garrity C, Garcia-Rovetta C, Rivas I, Delatorre U, Wong A, Kültz D et al. Tilapia Fish Skin Treatment of Third-Degree Skin Burns in Murine Model. Journal of Functional Biomaterials. 2023 Oct; 14(10): 512. doi: 10.3390/jfb14100512.
- [16] Abdelnaby A, Assar DH, Salah A, Atiba A, El-Nokrashy AM, Elshafey AE et al. Extracted Marine Collagen from Nile Tilapia (Oreochromis niloticus I.) Skin Accelerates Burn Healing: Histopathological,

- Immunohistochemical and Gene Expression Analysis. Egyptian Journal of Veterinary Sciences. 2025 Jul; 56(8): 1849-65. doi: 10.21608/ejvs.2024.290 709.2100.
- [17] Kaya M, Akdaşçi E, Eker F, Bechelany M, Karav S. Recent Advances of Silver Nanoparticles in Wound Healing: Evaluation of in Vivo and in Vitro Studies. International Journal of Molecular Sciences. 2025 Oct; 26(20): 9889. doi: 10.3390/ijms26209889.
- [18] Huang X, Liang P, Jiang B, Zhang P, Yu W, Duan M et al. Hyperbaric Oxygen Potentiates Diabetic Wound Healing by Promoting Fibroblast Cell Proliferation And Endothelial Cell Angiogenesis. Life sciences. 2020 Oct; 259: 118246. doi: 10.1016/j.lfs.2020.118246.
- [19] Barrera JA, Trotsyuk AA, Maan ZN, Bonham CA, Larson MR, Mittermiller PA et al. Adipose-Derived Stromal Cells Seeded in Pullulan-Collagen Hydrogels Improve Healing in Murine Burns. Tissue Engineering Part A. 2021 Jun; 27(11-12): 844-56. doi: 10.1089/ ten.tea.2020.0320.
- [20] Tang D, Lin Q, Li PW, Wang S, Xu K, Huang YS et al. FG-4592 Combined with PRP Significantly Accelerates the Healing of Refractory Diabetic Wounds by Upregulating HIF-1α. Scientific Reports. 2025 Apr; 15(1): 14292. doi: 10.1038/s41598-025-99356-3.
- [21] Chen R, Xu H, Li X, Dong J, Wang S, Hao J et al. Role of Oxidative Stress in Post-Burn Wound Healing. Burns and Trauma. 2025 Jun: tkaf040. doi: 10.1093/burnst/tkaf040.
- [22] Moreno DA, Saladini MS, Viroel FJ, Dini MM, Pickler TB, Amaral Filho J et al. Are Silver Nanoparticles Useful for Treating Second-Degree Burns? An Experimental Study in Rats. Advanced Pharmaceutical Bulletin. 2020 Nov; 11(1): 130. doi: 10.34172/apb.2021.014.
- [23] Matysiak-Kucharek M, Sawicki K, Kapka-Skrzypczak L. Effect of Silver Nanoparticles on Cytotoxicity, Oxidative Stress and Pro-Inflammatory Proteins Profile in Lung Adenocarcinoma A549 Cells. Annals of Agricultural and Environmental Medicine. 2023; 30(3): 566-9. doi: 10.26444/aaem/169214.
- [24] You C, Li Q, Wang X, Wu P, Ho JK, Jin R et al. Silver Nanoparticle Loaded Collagen/Chitosan Scaffolds Promote Wound Healing Via Regulating Fibroblast Migration and Macrophage Activation. Scientific Reports. 2017 Sep; 7(1): 10489. doi: 10.1038/s41598-017-10481-0.